

Access Point Deployment for Localizing Accuracy and User Rate in Cell-Free Systems

Fanfei Xu
Southeast University School of
Information Science and Engineering
Nanjing 210096, China

Shengheng Liu*
Southeast University School of
Information Science and Engineering
Nanjing 210096, China
s.liu@seu.edu.cn

Zihuan Mao
Southeast University School of
Information Science and Engineering
Nanjing 210096, China

Shangqing Shi
Southeast University School of
Information Science and Engineering
Nanjing 210096, China

Dazhuan Xu
Purple Mountain Laboratories
Nanjing 211111, China

Dongming Wang
Southeast University School of
Information Science and Engineering
Nanjing 210096, China

Yongming Huang*
Southeast University School of
Information Science and Engineering
Nanjing 210096, China

ABSTRACT

Evolving next-generation mobile networks is designed to provide ubiquitous coverage and networked sensing. With utility of multi-sensing and multi-node joint transmission, cell-free is a promising technique to realize this prospect. This paper aims to tackle the problem of access point (AP) deployment in cell-free systems to balance the sensing accuracy and user rate. By merging the D-optimality with Euclidean criterion, a novel integrated metric is proposed to be the objective function for both max-sum and max-min problems, which respectively guarantee the overall and lowest performance in multi-user communication and target tracking scenario. To solve the corresponding high dimensional non-convex multi-objective problem, the Soft actor-critic (SAC) is utilized to avoid risk of local optimal result. Numerical results demonstrate that proposed SAC-based APs deployment method achieves 20% of overall performance and 120% of lowest performance.

CCS CONCEPTS

• **Networks** → **Network performance modeling**; **Wireless access points, base stations and infrastructure**; • **Computing methodologies** → *Policy iteration*; • **Hardware** → **Wireless integrated network sensors**.

*Both authors are also affiliated to the Purple Mountain Laboratories, Nanjing 211111, China.

Permission to make digital or hard copies of all or part of this work for personal or classroom use is granted without fee provided that copies are not made or distributed for profit or commercial advantage and that copies bear this notice and the full citation on the first page. Copyrights for components of this work owned by others than the author(s) must be honored. Abstracting with credit is permitted. To copy otherwise, or republish, to post on servers or to redistribute to lists, requires prior specific permission and/or a fee. Request permissions from permissions@acm.org.
ACM MobiCom '24, November 18–22, 2024, Washington D.C., DC, USA
© 2024 Copyright held by the owner/author(s). Publication rights licensed to ACM.
ACM ISBN 979-8-4007-0489-5/24/11
<https://doi.org/10.1145/3636534.3698221>

KEYWORDS

Cell-free, integrated sensing and communication, access point deployment, soft actor-critic, deep reinforcement learning

ACM Reference Format:

Fanfei Xu, Shengheng Liu, Zihuan Mao, Shangqing Shi, Dazhuan Xu, Dongming Wang, and Yongming Huang. 2024. Access Point Deployment for Localizing Accuracy and User Rate in Cell-Free Systems. In *The 30th Annual International Conference on Mobile Computing and Networking (ACM MobiCom '24)*, November 18–22, 2024, Washington D.C., DC, USA. ACM, New York, NY, USA, 7 pages. <https://doi.org/10.1145/3636534.3698221>

1 INTRODUCTION

The integrated sensing and communication (ISAC) is expected to become a key usages scenario of the future six-th generation (6G) networks, which is mentioned in newest recommendation concerned with framework and objective of future network of the International Telecommunication Union [10]. Telecommunication base stations, as a widely deployed infrastructure, can significantly enhance situational awareness when equipped with radar sensing capabilities, enabling a variety of novel applications, such as low-altitude drone intrusion detection and accurate virtual environment construction for digital twins [12]. Moreover, as wireless communication networks continue to evolve towards higher frequency bands, more spectrum resources can be obtained to satisfy the high bandwidth requirements of sensing functions. However, high-frequency signals with poor diffraction and high attenuation, makes traditional single station sensing performance significantly limited to shadow effects of obstructions.

Cell-free networks [9, 14], an innovative architecture for 6G networks, may tackle this issue. Unlike conventional cellular networks, where each user equipment (UE) is served by a single base station within a designated cell, cell-free networks deploy a large number of distributed access points (APs) that collaboratively serve all users within the area. Widely-spread APs connected to a central processing unit (CPU) enable seamless sensing and ubiquitous coverage by use of key techniques such as dynamic user association and

APs deployment [1]. Different APs location seriously affects the channel condition, intuitively, to fully leverage the advantages such as multi-view sensing information and joint transmission of the cell-free ISAC systems, investigating optimal APs deployment is vitally necessary.

Mathematical solutions such as vector quantization and gradient descent [2, 4, 13] were proposed to optimize the two dimension (2D) location of APs to improve of spectral efficiency in cell-free networks. On-demand service capability concerned with sum throughput was achieved by solving APs deployment [7] based on multiple linear regression model. Moreover, APs deployment not only affects communication performance, but also impacts sensing performance. Cramér-Rao lower bound (CRLB) was developed [6] for target velocity estimation in multiple-input multiple output (MIMO) radar, shown that the antenna placement affects the estimation accuracy significantly. Also in MIMO radar systems [3], CRLB for target localization in both coherent and non-coherent processing was developed. Additionally, based on the best unbiased linear unbiased estimator it derived, a closed-form localization estimation that revealed the relationship between antennas location, target location, and localization accuracy was provided. Furthermore, geometry gain of antennas deployment for target localizing is [11] analyzed in MIMO radar systems. In summary, substantial researches have separately analyzed the impacts of APs deployment on communication and sensing performance. However, the area of jointly considering both of them still remains blank.

Thus, to simultaneously measure sensing and communication performance, in this work we propose a unified evaluation metric in cell-free ISAC systems, merging user rate with localizing accuracy [8] derived from Euclidean distance and D-optimal criterion, and utilize it as the objective function for APs deployment optimization. In addition, considering fairness for all UEs and localizing accuracy throughout the target moving trajectory, we provide the deployment results of both max-sum and max-min problem. Due to the non-convex and high-dimensional property of the original multi-objective problem, mathematical algorithms are challenging to solve it. Soft actor-critic (SAC) [5], a deep reinforcement learning (DRL) based APs deployment method is proposed, with the utility of additive maximum AP deployment entropy term to avoid local optimum. Numerical results show the superior performance of our proposed SAC-based deployment method compared with other DRL algorithms such as deep deterministic policy gradient (DDPG) and twin-delayed DDPG (TD3).

2 ISAC SIGNAL MODEL AND PROBLEM FORMULATION

As illustrated in Fig. 1, we consider a cell-free ISAC system consists of M single-antenna transmitter APs and N single-antenna receiver APs which collaboratively serve K single-antenna UEs and estimate position of one target moving with specific trajectory. The 2D position of them is denoted by $\mathbf{t}_m = [x_m^t, y_m^t]$, $\mathbf{r}_n = [x_n^r, y_n^r]$, $\mathbf{u}_k = [x_k, y_k]$, $\mathbf{p} = [x^p, y^p]$ respectively, where $m \in \mathbb{M} = \{1, \dots, M\}$, $n \in \mathbb{N} = \{1, \dots, N\}$, $k \in \mathbb{K} = \{1, \dots, K\}$.

2.1 Fisher Information

When system is executing sensing function module, M transmitting APs send probe signal and N receiving APs capture the echo from

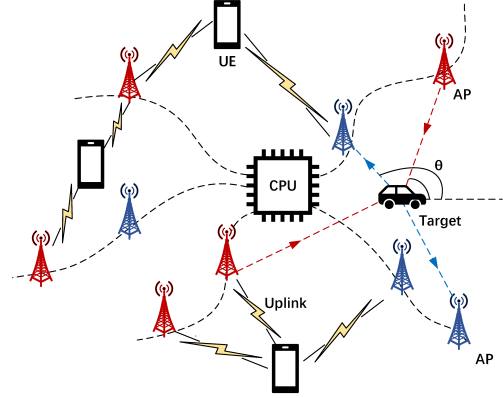


Figure 1: Cell-free ISAC systems.

target. In this distributed detection system, the low-pass equivalent of the narrow-band signal transmitted from i -th APs at time t is represented as $\sqrt{E/M}s_i(t)$, where E denotes the total transmission energy. We assume that the transmission signal is uncorrelated in any time delay,

$$\int_T s_i(t)s_j^*(t-\tau)dt \approx \begin{cases} 1, & \text{if } i = j \\ 0, & \text{if } i \neq j, \end{cases} \quad (1)$$

where $(\cdot)^*$ represent the conjugate operator. In addition, the signal is normalized in the whole signal processing interval T , i.e., $\int_T |s_i(t)|^2 dt = 1$.

Non-coherent processing, a more practical operation is selected due to its low requirement of time synchronization compared with coherent processing. The echo signal accepted at n -th receiving AP is denoted by

$$y_n(t) = \sum_{m=1}^M \eta_{mn} s_m(t - \tau_{mn}) + w_n(t), \quad (2)$$

where $w_n(t) \stackrel{\text{i.i.d.}}{\sim} \mathcal{CN}(0, 1)$ represents additive Gaussian noise, $\eta = [\eta_{11}, \eta_{12}, \dots, \eta_{mn}, \dots, \eta_{MN}]^T$ is the coefficient referring to target reflection and channel propagation fading. τ_{mn} denotes time delay of signal transmission and reflection between m -th transmitting AP and n -th receiving AP

$$\tau_{mn} = \frac{d_m + d_n}{c}, \quad (3)$$

where c is speed of light and $d_m = \|\mathbf{t}_m - \mathbf{p}\|_2$, $d_n = \|\mathbf{r}_n - \mathbf{p}\|_2$ denote the distance between target \mathbf{p} and transmitter or receiver AP.

As for the localizing accuracy, we utilize D-optimal criterion to evaluate the performance of parameter estimation. The product of the CRLB matrix eigenvalues (or determinant) is minimize, which is equivalent to minimize the area of the Elliptical error probable. Fisher information matrix (FIM) is the inverse of CRLB matrix, therefore, minimizing the determinant of CRLB matrix converts to maximizing the FIM. The FIM of the estimation for the parameter

vector ϑ by use of the measurement vector \mathbf{x} can be expressed as:

$$\Phi = \mathbb{E} \left\{ \left[\frac{\partial}{\partial \vartheta} \ln f(\mathbf{x}|\vartheta) \right] \left[\frac{\partial}{\partial \vartheta} \ln f(\mathbf{x}|\vartheta) \right]^T \right\}. \quad (4)$$

To be specific, when the error of the estimation is Gaussian noise, the FIM for in cell-free ISAC system, non-coherent sensing FIM for target detection is equal to

$$\Phi = \begin{bmatrix} \phi_{11} & \phi_{12} \\ \phi_{21} & \phi_{22} \end{bmatrix} = \mathbf{J}_0^T \Sigma^{-1} \mathbf{J}_0, \quad (5)$$

where \mathbf{J}_0 is the Jacobian matrix of the target localizing at $\mathbf{p} = [x^p, y^p]$

$$\mathbf{J}_0 = [(\alpha_1^t + \alpha_1^r) (\alpha_1^t + \alpha_2^r) \cdots (\alpha_1^t + \alpha_N^r) \cdots (\alpha_M^t + \alpha_N^r)]^T, \quad (6)$$

where $\alpha_m^t = [\cos \theta_m^t \sin \theta_m^t]^T$, $\alpha_n^r = [\cos \theta_n^r \sin \theta_n^r]^T$, θ represents the bearing angle of the AP relative to the target, measured from the horizontal axis. According to [11], the expression of determinant of the angular FIM is

$$|\Phi| = \left\{ \sum_{m=1}^M \sum_{n=1}^N (\cos \theta_m^t + \cos \theta_n^r)^2 \sum_{m=1}^M \sum_{n=1}^N (\sin \theta_m^t + \sin \theta_n^r)^2 - \left[\sum_{m=1}^M \sum_{n=1}^N (\cos \theta_m^t + \cos \theta_n^r) (\sin \theta_m^t + \sin \theta_n^r) \right]^2 \right\}. \quad (7)$$

Next, we transform the determinant of the angular FIM into two-dimensional Cartesian coordinates, and determine optimal APs deployment positions based on the maximum value of the FIM determinant.

$$|\Phi| = \left\{ \sum_{m=1}^M \sum_{n=1}^N \left(\frac{x^p - x_m^t}{\|\mathbf{p} - \mathbf{t}_m\|_2} + \frac{x^p - x_n^r}{\|\mathbf{p} - \mathbf{r}_n\|_2} \right)^2 \sum_{m=1}^M \sum_{n=1}^N \left(\frac{y^p - y_m^t}{\|\mathbf{p} - \mathbf{t}_m\|_2} + \frac{y^p - y_n^r}{\|\mathbf{p} - \mathbf{r}_n\|_2} \right)^2 - \left[\sum_{m=1}^M \sum_{n=1}^N \left(\frac{x^p - x_m^t}{\|\mathbf{p} - \mathbf{t}_m\|_2} + \frac{x^p - x_n^r}{\|\mathbf{p} - \mathbf{r}_n\|_2} \right) \left(\frac{y^p - y_m^t}{\|\mathbf{p} - \mathbf{t}_m\|_2} + \frac{y^p - y_n^r}{\|\mathbf{p} - \mathbf{r}_n\|_2} \right) \right]^2 \right\}. \quad (8)$$

2.2 User Sum Rate

A cell-free uplink communication model is studied in this section, where all $M + N$ APs simultaneously accept signals from all K UEs. The uplink receiving signal at l -th AP is

$$y_l = \sum_{k=1}^K \sqrt{\rho} h_{lk} x_k + w_l, \quad (9)$$

where $\sqrt{\rho}$, x_k is transmitter power and data symbol of k -th UE, $l \in \{1, 2, \dots, M + N\}$. The received signal of all $M + N$ APs can be represented as

$$\mathbf{y} = \sqrt{\rho} \mathbf{H} \mathbf{x} + \mathbf{w}, \quad (10)$$

where $\mathbf{x} = [x_1, x_2, \dots, x_K]^T$, $\mathbf{w} = [w_1, w_2, \dots, w_{M+N}]^T$ and $\mathbf{H}[l, k] = h_{lk}$, $\mathbf{H} \in \mathbb{C}^{(M+N) \times K}$ is channel coefficients matrix. The narrow-band fading channel coefficient is written as $h_{lk} = \sqrt{\beta_{lk}} g_{lk}$, where $g_{lk} \stackrel{\text{i.i.d.}}{\sim} \mathcal{CN}(0, 1)$ small fading coefficients, and β_{lk} is large fading coefficients

$$\beta_{lk} = \begin{cases} \frac{d_0}{\|\mathbf{t}_l - \mathbf{u}_k\|_2^2}, & \text{if } l \leq M \\ \frac{d_0}{\|\mathbf{r}_l - \mathbf{u}_k\|_2^2}, & \text{if } M < l \leq M + N, \end{cases} \quad (11)$$

where d_0 is a constant denoting the reference distance.

In cell-free systems, signals accepted by distributed APs at various geographic position can be collectively processed in CPU. For instance, zero forcing reception is employed to mitigate interference from multiple UEs. Then, the processed received signal is expressed as

$$\hat{\mathbf{y}} = (\mathbf{H}^H \mathbf{H})^{-1} \mathbf{H}^H \mathbf{y}. \quad (12)$$

The asymptotic SNR can be expressed as

$$\frac{1}{M + N} \text{SNR}_k \xrightarrow[(M+N) \rightarrow \infty]{a.s.} \rho \bar{\beta}_k, \quad (13)$$

where $\bar{\beta}_k \triangleq \lim_{(M+N) \rightarrow \infty} \frac{1}{M+N} \sum_l \beta_{lk}$. For simplification of derivation, we consider the transmit power to be unity for all UEs. We assume no shadow fading in the large-scale fading coefficient β_{lk} , and constant d_0 is 1. These assumptions do not affect the conclusions of subsequent methods. At this point, the SNR for k UE can be expressed by use of Euclidean distance criterion:

$$\text{SNR}_k = \left(\sum_{m=1}^M \frac{1}{\|\mathbf{u}_k - \mathbf{t}_m\|_2^2} + \sum_{n=1}^N \frac{1}{\|\mathbf{u}_k - \mathbf{r}_n\|_2^2} \right). \quad (14)$$

The sum communication rate of cell-free systems is

$$\begin{aligned} \sum_{k=1}^K R_k &= \sum_{k=1}^K \log(1 + \text{SNR}_k) \\ &= \sum_{k=1}^K \log \left(\sum_{m=1}^M \frac{1}{\|\mathbf{u}_k - \mathbf{t}_m\|_2^2} + \sum_{n=1}^N \frac{1}{\|\mathbf{u}_k - \mathbf{r}_n\|_2^2} \right). \end{aligned} \quad (15)$$

2.3 Deployment Problem Formulation

In the context of cell-free ISAC systems, the comprehensive consideration of communication and sensing performance can be modeled as a multi-objective optimization problem

$$\begin{aligned} \max_{\mathbf{t}, \mathbf{r}} \quad & U(\mathbf{t}, \mathbf{r}) = (U_1, U_2) \\ \text{s.t.} \quad & x_{\min} \leq x_i(x) \leq x_{\max}, \quad i = 1, \dots, M + N \\ & y_{\min} \leq y_i(x) \leq y_{\max}, \quad i = 1, \dots, M + N, \end{aligned} \quad (16)$$

constraints in (16) mean that all APs must be deployed within a specific area.

Directly solving the Pareto front of multi-objective problems is highly challenging. Therefore, we transform the original problem into a single-objective optimization problem for solution.

Due to the dimensional disparity between localizing accuracy and communication rate, traditional weighted sum approaches struggle to achieve balanced optimization between the two. Therefore, we adopt a multiplication method to transform the original problem for resolution, thereby achieving a better trade-off between communication and sensing performance.

We firstly consider the maximizing sum of communication capacity and sensing accuracy during the target moving trajectory. In addition, to ensure the uniform service for all UEs and sensing accuracy throughout the entire trajectory period, we also consider the maximization of minimum capacity and accuracy. Then, the

objective function can be represented as

$$U(\mathbf{t}, \mathbf{r}) = \begin{cases} \sum_{k=1}^K R_k / Q \cdot \sum_{\mathbf{p}(\epsilon)} |\Phi| / Q, & \text{for max-sum} \\ \min_{k \in \mathbb{K}} R_k \cdot \min_{\mathbf{p}(\epsilon)} |\Phi|, & \text{for max-min.} \end{cases} \quad (17)$$

where $\mathbf{p}(\epsilon)$ denotes the parametric expression of the moving target trajectory. $Q = \text{card}(\epsilon)$ is the sample point number of trajectory.

3 SOFT ACTOR CRITIC BASED AP DEPLOYMENT

Considering the original problem involving the multiplication of multiple objective functions is a complex non-convex optimization problem, traditional mathematical methods struggle to achieve the optimal solution. Thus, we first transform the problem into a Markov decision process (MDP) and utilize SAC for its solution. Compared to traditional deep reinforcement learning algorithms, SAC introduces a maximum entropy term in the loss function, which enhances its exploratory performance and mitigates the risk of falling into local optimal solution. This characteristic makes SAC particularly well-suited for addressing the complex multi-objective AP deployment problem.

3.1 MDP Formulation

Our MDP is represented by a tuple $(\mathbb{S}, \mathbb{A}, P, R)$, compared with traditional SAC, both state \mathbb{S} and action \mathbb{A} are discretized here to reduce the complexity of the exploration space and accelerate training procedure. $P: \mathbb{S} \times \mathbb{S} \times \mathbb{A} \rightarrow [0, \infty)$ is the state transition probability density function to the next state $s_{i+1} \in \mathbb{S}$ given current state $s_i \in \mathbb{S}$ and action $a_i \in \mathbb{A}$. After taking action, the agent gets reward $r(s_i, a_i) \in \mathbb{R}$ according to the reward function $R: \mathbb{S} \times \mathbb{A} \rightarrow \mathbb{R}$. The specific designs of states, actions, and rewards in our APs deployment problem are as follows.

- State: Since the optimal deployment positions of APs are greatly relying on user and target positions, the state space is defined by the two-dimensional coordinates of users and targets.

$$\mathbf{s}_i = \{\mathbf{u}_1, \dots, \mathbf{u}_K, \mathbf{p}\}. \quad (18)$$

- Action: As mentioned in Section II, in our cell-free ISAC networks, the communication capacity and sensing accuracy are both related to the locations APs. Intuitively, we consider representing the action space using the 2D coordinates of APs.

$$\mathbf{a}_i = \{\mathbf{t}_1^i, \dots, \mathbf{t}_M^i, \mathbf{r}_1^i, \dots, \mathbf{r}_N^i\}. \quad (19)$$

- Reward: The form of the reward function is determined by the expression of the objective function.

$$r(\mathbf{s}_i, \mathbf{a}_i) = \begin{cases} \sum_{k=1}^K R_k \cdot \sum_{\mathbf{p}(\epsilon)} |\Phi|, & \text{for max-sum} \\ \min_{k \in \mathbb{K}} R_k \cdot \min_{\mathbf{p}(\epsilon)} |\Phi|, & \text{for max-min.} \end{cases} \quad (20)$$

3.2 SAC for Deployment

Traditional DRL is aiming to learn the optimal policy π which maximizes the cumulative expected rewards, whereas SAC adds a maximum policy entropy term in the DRL objective function

$$C(\pi) = \sum_i E_{(\mathbf{s}_i, \mathbf{a}_i) \sim \rho_\pi} [r(\mathbf{s}_i, \mathbf{a}_i) + \omega \mathcal{H}(\pi(\cdot | \mathbf{s}_i))], \quad (21)$$

where π represents the policy generated by actor network, ρ_π is the historical state-action trajectory under the policy π , ω is a weighting parameter called temperature coefficient that balances the exploration and exploiting historical experience during the training procedure. $\mathcal{H}(\pi(\cdot | \mathbf{s}_i)) = -\log \pi(\cdot | \mathbf{s}_i)$ is the entropy of action policy at state \mathbf{s}_i .

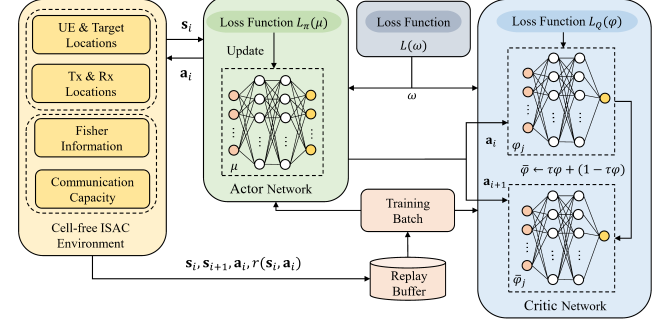


Figure 2: Architecture of SAC-based cell-free ISAC APs deployment system.

As shown in Fig. 2, the architecture of SAC-based cell-free ISAC APs deployment systems mainly contains three component. The first component is the training environment, responsible for receiving and executing actions from the actor network. Upon completion of execution, it generates the reward value for current state-action pair and transits to the next state, while storing corresponding state transition historical experience in the replay buffer \mathcal{B} for neural network updates. The second part is the SAC actor network, denoted by parameters μ , with its loss function defined as follows

$$L_\pi(\mu) = E_{\mathbf{s}_i \sim \mathcal{B}} \left[E_{\mathbf{a}_i \sim \pi_\mu} [\omega \log(\pi_\mu(\mathbf{a}_i | \mathbf{s}_i)) - Q_\varphi(\mathbf{s}_i, \mathbf{a}_i)] \right]. \quad (22)$$

The actor network generates action vectors corresponding to input state vectors and feeds them back to the environment for execution. Additionally, the critic network also requires the action vector when updating the Bellman equation.

The third component is the critic network parameterized by φ , with the loss function expressed as follows

$$L_Q(\varphi) = E_{(\mathbf{s}_i, \mathbf{a}_i) \sim \mathcal{B}} \left[\frac{1}{2} (Q_\varphi(\mathbf{s}_i, \mathbf{a}_i) - (r(\mathbf{s}_i, \mathbf{a}_i) + \gamma Q_{\bar{\varphi}}(\mathbf{s}_{i+1}, \mathbf{a}_{i+1}) - \log \pi_\mu(\mathbf{a}_{i+1} | \mathbf{s}_{i+1})))^2 \right], \quad (23)$$

where γ is discount factor.

The critic network takes a state-action pair as input and outputs a Q-value used to assess the quality of the action taken in the current state, where a higher Q-value indicates the potential for greater cumulative reward. In contrast to the original critic network φ , the target critic network $\bar{\varphi}$ generates state-action pair for the next state, which is used in updating the Bellman equation. To mitigate training instability caused by overly large Q-value estimates, both φ_j and $\bar{\varphi}_j$, $j \in \{1, 2\}$ maintain two networks and utilize the smaller Q-value for network updates. A soft update strategy $\bar{\varphi} \leftarrow \tau\varphi + (1-\tau)\bar{\varphi}$ with $\tau \ll 1$ is employed.

In addition to these three main components, another important parameter, the temperature coefficient ω , is also automatically updated according to its loss function

$$L(\omega) = E_{\mathbf{a}_i \sim \pi_\mu} \left[-\omega_i \log \pi_\mu(\mathbf{a}_i | \mathbf{s}_i) - \omega_i \overline{\mathcal{H}} \right], \quad (24)$$

where $\overline{\mathcal{H}} = -|\mathcal{A}|_{\dim}$ represents the predefined lower bound of the action policy entropy.

4 SIMULATION

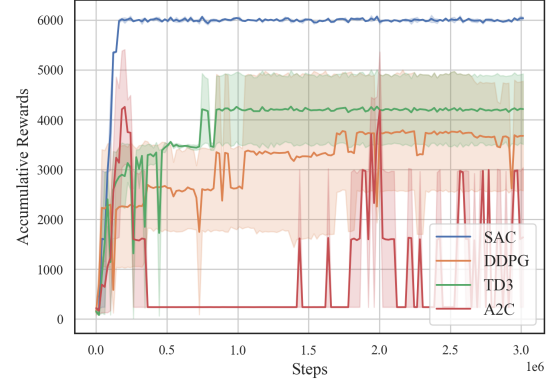
Table 1: Parameters in DRL model

Parameters	values
Hidden layer	64×32
Learning rate	10^{-5}
Buffer size	2^{21}
Batch size	2^9
Discount factor γ	0.98
Soft update target critic network τ	0.005

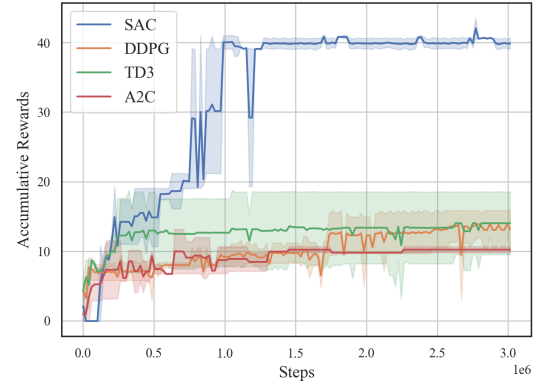
In this section, we evaluated the performance of our proposed SAC-based APs deployment method in cell-free ISAC systems. We demonstrated the superiority of SAC in this scenario through comparisons with several traditional DRL algorithms. Additionally, to validate the effectiveness of optimizing the joint communication and sensing metric proposed in this work, we compared it with results of only sensing optimizing, only communication optimizing, and weighted sum of communication and sensing optimizing. The configuration of DRL Model is show in Table 1. In our cell-free systems, the target moves along a predefined circular trajectory, while three UEs distributed around the target follow Gaussian distributions with a variance of 2. During sensing tasks, receiving APs capture echoes transmitted from transmitting AP, reflected from the target. During communication tasks, all APs jointly receive uplink signals from all UEs.

As shown in Fig. 3, in cell-free ISAC systems, the final convergence result of our proposed SAC-based algorithm significantly surpasses other traditional DRL algorithms in both max-min and max-sum problem. Also, SAC is more stable under different random seeds compared with other algorithms. The hyperparameters of DDPG and TD3 exert a profound impact on their performance, typically, for a complex optimization problem, finding hyperparameters that enable them to exceeds the performance of SAC is challenging. According to the data in Table 2, an increase in the number of APs is observed to correlate positively with improved ISAC performance, thereby significantly demonstrating the pronounced advantage of the cell-free systems in this regard.

To be more specific, Fig. 4 and Fig. 5 depict the APs deployment results of the cell-free ISAC systems using different algorithms in max-sum and max-min problems. According to the D-optimal criterion, optimal sensing performance is achieved when the positions of transmitting APs and receiving APs lie on a straight line and form specific angles with the target. According to the Euclidean distance criterion derived from zero-forcing reception, communication performance improves as APs approach to UEs. SAC-based



(a)



(b)

Figure 3: Accumulative ISAC rewards of different DRL Algorithms. (a) Max-sum problem. (b) Max-min problem.

Table 2: ISAC value of different number of APs

Number of APs (M+N)	2	4	6	8
$\sum_{k=1}^K R_k / Q \cdot \sum_{\mathbf{p}(\epsilon)} \Phi / Q$	41.07	775.73	3804.47	11614.07
$\min_{k \in \mathbb{K}} R_k \cdot \min_{\mathbf{p}(\epsilon)} \Phi $	0.042	10.48	86.06	257.28

APs deployment result satisfies both sensing and communication criterion well. Furthermore, APs deployment in max-min problem in Fig. 5(a) shows that to ensure fairness in service among UEs, each UE is surrounded by several nearby APs to achieve higher SNR. In contrast, in the deployment result of the max-sum problem in Fig. 4(a), all APs are concentrated around the UEs closest to the optimal sensing position.

Table 3 illustrates the communication and sensing values under optimal APs deployment in different objective functions. In both max-min and max-sum problem, the communication values of our

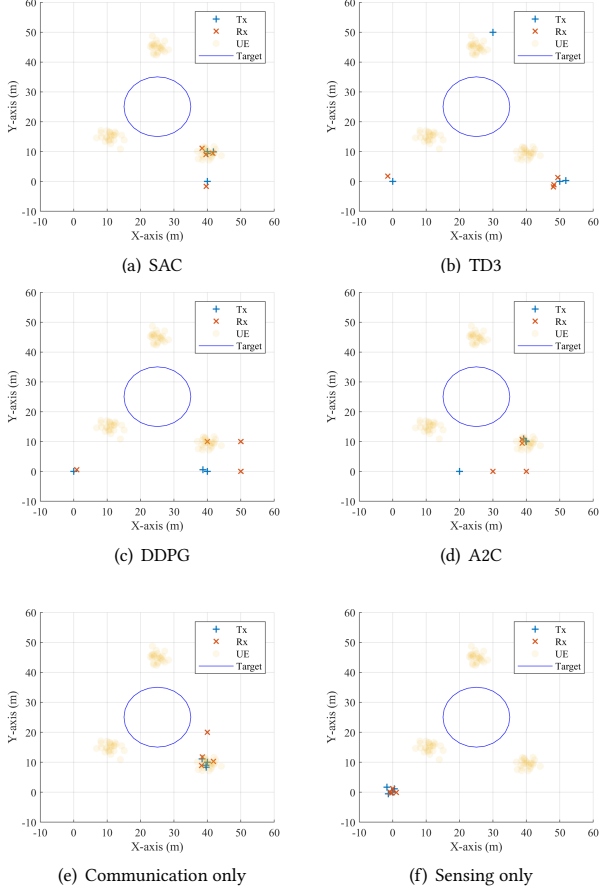


Figure 4: APs deployment results of max-sum problem.

Table 3: Communication rate and localizing accuracy of different objective

Objective	ISAC	Sensing only	Comm. only	Weighted sum
$\sum_{k=1}^K R_k/Q$	1.13	0.014	1.26	0.015
$\sum \Phi /Q$	688.97	842.92	642.08	842.92
$\min_{k \in \mathbb{K}} R_k$	0.042	0.0013	0.043	0.0013
$\min \Phi $	0.25	696.89	188.40	696.89

ISAC optimization is almost equal to the result of only optimizing the communication objective, and far higher than only optimizing sensing method, while the sensing values of ISAC optimization is better than communication method but lower than sensing-only method. This is because the optimal APs deployment position for sensing are typically aligned in a straight line at specific angles with the target. However, UEs distribution usually does not conform to this characteristic. Therefore, to balance communication rate of UEs, APs cannot be deployed at the optimal sensing position, resulting

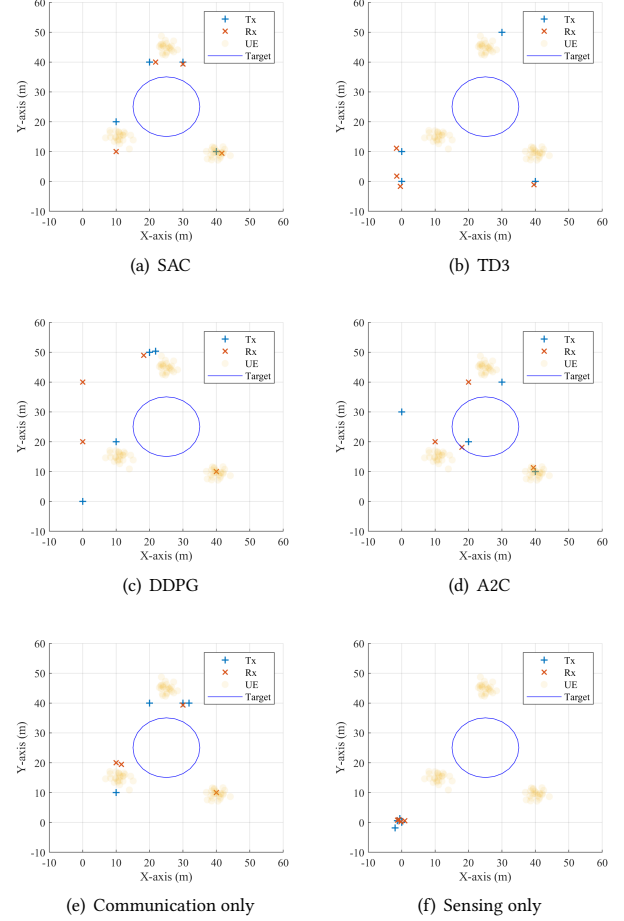


Figure 5: APs deployment results of max-min problem.

in a sacrifice of some sensing performance. In addition, due to the significantly different magnitudes between sensing accuracy and communication rate, finding a balanced weight in their sum as a objective function proves challenging. It can be observed that the result of weighted sum method is nearly equivalent to optimizing sensing performance alone.

Fig. 4(f) and Fig. 5(f) presents the deployment results of optimizing communication alone and optimizing sensing alone. As previously analyzed, for optimal sensing performance, APs form a line with target at a specific angles. For optimal communication performance, as shown in Fig. 4(e) and Fig. 5(e), APs strive to be as close to the UEs as possible to achieve higher SNR.

5 CONCLUSION

In this work, we have firstly investigated the APs deployment problem for maximizing user rate and localizing accuracy in the cell-free ISAC systems. Then a unified evaluation metric merging D-optimal criterion with Euclidean distance have been designed, which enables simultaneous optimization of communication and sensing performance. Finally, we have employed SAC, a DRL algorithm

augmented with maximum action policy entropy to solve the original non-convex and high-dimensional problem. Numerical findings demonstrated superior convergence results of the proposed method compared with other DRL methods for both system overall performance and fairness performance.

ACKNOWLEDGMENTS

This work was supported in part by the Fundamental Research Funds for the Central Universities under Grant Nos. 2242022k60002 and 2242023R40005.

REFERENCES

- [1] Hussein A. Ammar, Raviraj Adve, Shahram Shahbazpanahi, Gary Boudreau, and Kothapalli Venkata Srinivas. 2022. User-Centric Cell-Free Massive MIMO Networks: A Survey of Opportunities, Challenges and Solutions. *IEEE Communications Surveys and Tutorials* 24, 1 (2022), 611–652. <https://doi.org/10.1109/COMST.2021.3135119>
- [2] Carles Diaz-Vilor, Angel Lozano, and Hamid Jafarkhani. 2024. Cell-Free UAV Networks With Wireless Fronthaul: Analysis and Optimization. *IEEE Transactions on Wireless Communications* 23, 3 (2024), 2054–2069.
- [3] Hana Godrich, Alexander M. Haimovich, and Rick S. Blum. 2010. Target Localization Accuracy Gain in MIMO Radar-Based Systems. *IEEE Transactions on Information Theory* 56, 6 (2010), 2783–2803. <https://doi.org/10.1109/TIT.2010.2046246>
- [4] Govind R. Gopal and Bhaskar D. Rao. 2024. Vector Quantization Methods for Access Point Placement in Cell-Free Massive MIMO Systems. *IEEE Transactions on Wireless Communications* 23, 6 (2024), 5425–5440. <https://doi.org/10.1109/TWC.2023.3326453>
- [5] Tuomas Haarnoja, Aurick Zhou, Kristian Hartikainen, George Tucker, Sehoon Ha, Jie Tan, Vikash Kumar, Henry Zhu, Abhishek Gupta, Pieter Abbeel, et al. 2018. Soft actor-critic algorithms and applications. *arXiv preprint arXiv:1812.05905* (2018).
- [6] Qian He, Rick S. Blum, Hana Godrich, and Alexander M. Haimovich. 2008. Cramer-Rao bound for target velocity estimation in MIMO radar with widely separated antennas. In *2008 42nd Annual Conference on Information Sciences and Systems*. 123–127. <https://doi.org/10.1109/CISS.2008.4558507>
- [7] Jing Jiang, Fengyang Yan, Yinghui Ye, Worakrin Sutthiphpan, Jiayi Zhang, and Bo Ai. 2023. Traffic Demand-Oriented Cell-Free Massive MIMO Network. *IEEE Wireless Communications Letters* 12, 11 (2023), 1861–1865. <https://doi.org/10.1109/LWC.2023.3296527>
- [8] An Liu, Zhe Huang, Min Li, Yubo Wan, Wenrui Li, Tony Xiao Han, Chenchen Liu, Rui Du, Danny Kai Pin Tan, Jianmin Lu, Yuan Shen, Fabiola Colone, and Kevin Chetty. 2022. A Survey on Fundamental Limits of Integrated Sensing and Communication. *IEEE Communications Surveys & Tutorials* 24, 2 (2022), 994–1034. <https://doi.org/10.1109/COMST.2022.3149272>
- [9] Hien Quoc Ngo, Alexei Ashikhmin, Hong Yang, Erik G. Larsson, and Thomas L. Marzetta. 2017. Cell-Free Massive MIMO Versus Small Cells. *IEEE Transactions on Wireless Communications* 16, 3 (2017), 1834–1850.
- [10] ITU-R Recommendation. 2023. Framework and overall objectives of the future development of IMT for 2030 and beyond. *International Telecommunication Union (ITU) Recommendation (ITU-R)* (2023).
- [11] Mohammad Sadeghi, Fereidoon Behnia, Rouhollah Amiri, and Alfonso Farina. 2021. Target Localization Geometry Gain in Distributed MIMO Radar. *IEEE Transactions on Signal Processing* 69 (2021), 1642–1652. <https://doi.org/10.1109/TSP.2021.3062197>
- [12] Zhiqing Wei, Yucong Du, Qixun Zhang, Wangjun Jiang, Yanpeng Cui, Zeyang Meng, Huici Wu, and Zhiyong Feng. 2024. Integrated Sensing and Communication Driven Digital Twin for Intelligent Machine Network. *IEEE Internet of Things Magazine* 7, 4 (2024), 60–67. <https://doi.org/10.1109/IOTM.001.2300214>
- [13] Fanfei Xu, Yuhuan Ruan, and Yongzhao Li. 2023. Soft Actor-Critic Based 3-D Deployment and Power Allocation in Cell-Free Unmanned Aerial Vehicle Networks. *IEEE Wireless Communications Letters* 12, 10 (2023), 1692–1696. <https://doi.org/10.1109/LWC.2023.3288273>
- [14] Xiaohu You, Yongming Huang, Shengheng Liu, et al. 2023. Toward 6G TKμ extreme connectivity: Architecture, key technologies and experiments. *IEEE Wireless Communications* 30, 3 (2023), 86–95. <https://doi.org/10.1109/MWC.004.2200482>

Received XX XXXX 2024; revised XX XXXX 2024; accepted XX XXXX 2024